Effect of supercritical CO2 and olive leaf extract on the structural, thermal and mechanical properties of an impregnated food packaging film

This is the Accepted version of the following publication

Cejudo-Bastante, Cristina, Cran, Marlene, Casas Cardoso, Lourdes, Mantell-Serrano, Casimiro, Martínez de la Ossa, Enrique José and Bigger, Stephen W (2019) Effect of supercritical CO2 and olive leaf extract on the structural, thermal and mechanical properties of an impregnated food packaging film. Journal of Supercritical Fluids, 145. pp. 181-191. ISSN 0896-8446

The publisher’s official version can be found at
https://www.sciencedirect.com/science/article/pii/S089684461830528X?via%3Dihub
Note that access to this version may require subscription.

Downloaded from VU Research Repository https://vuir.vu.edu.au/38169/

Effect of Supercritical CO_2 and Olive Leaf Extract on the Structural, Thermal and Mechanical Properties of an Impregnated Food Packaging Film

C. Cejudo Bastante*[a], M. J. Cran[b], L. Casas Cardoso[a], C. Mantell Serrano[a], E. J. Martínez de la Ossa[a],
S. W. Bigger[b]

[a]Chemical Engineering and Food Technology Department, Wine and Agrifood Research Institute (IVAGRO), University of Cadiz, Cádiz, Spain

[b]Institute for Sustainable Industries and Liveable Cities, Victoria University, Melbourne, Australia

*corresponding author: Cristina Cejudo Bastante (cristina.cejudo@uca.es)

Abstract (150 words)

Poly(ethylene terephthalate)/polypropylene (PET/PP) films containing olive leaf extract (OLE) were obtained by supercritical solvent impregnation (SSI) in batch (BM) and semi-continuous (SM) modes. The study focused on the impact of pressure, temperature, CO_2 flow and OLE on the properties of the impregnated films. Thermal analysis of non-impregnated samples revealed a decrease in the crystallinity of PP layer treated at 35 ºC and an increase in the T_g of PET treated at 55 ºC due to CO_2 sorption. In impregnated samples, high pressures caused a decrease in the crystallinity of PP layer, whereas PET layer remained unaffected. Higher pressures favour impregnation in BM, whereas different trends were found for SM impregnations. Although the film properties were not compromised after impregnation, the CO_2 stream used in SM slightly weakened the impregnated films. Overall, conditions of 400 bar and 35ºC in BM were favorable for producing highly antioxidant films with minor structural modifications.

Keywords (6): PET/PP multilayer film; supercritical impregnation; olive leaf extract; active packaging; film properties

1. Introduction

The demand for minimally processed foods without additives is ever increasing and one of the more innovative alternatives is the inclusion of preservatives in food packaging materials. The use of natural antioxidant compounds (AOs) in packaging films offers some advantages compared to the direct addition of preservatives to the foodstuff. These include the need for lower amounts of active compounds to impart AO activity, the potential for the controlled release to the food matrix, and confining the AO activity to the product surface [1].

In the food packaging field, there is usually no single material that has all the requirements for the conservation of a specific product and so the combination of different materials is often used to optimize the packaging. Multilayer films have thus gained attention due to these providing certain mechanical, barrier or heat-sealing properties that monolayer films cannot offer [2, 3]. Multilayer films have been used for creating AO or antimicrobial (AM) packaging using polymers alone or in combination with other materials such as paper or fibers [4-7]. Among them, low- and high-density polyethylene (LDPE and HDPE), ethylene-vinyl acetate (EVA), poly(lactic acid) films (PLA), poly(ethylene terephthalate) (PET) or polypropylene (PP) are commonly used as substrates in active packaging material. In particular, PET has been used in coatings and multilayer formulations for obtaining an oxygen barrier material [8-11], whereas PP has been used in anti-insect and AM packaging material [12, 13].

Although procedures such as extrusion or coating have been used traditionally for developing active packaging, supercritical solvent impregnation (SSI) using CO_2 offers numerous advantages compared with other practices due to its mild critical point conditions (31.06 °C and 73.8 bar), high diffusivity, low viscosity and inert nature among other factors [14]. It is also possible to impregnate both non-polar and polar compounds (whether adding low amounts of polar solvents) and control the loading extent by modifying the operating parameters such as pressure, time, temperature or depressurization rate [15]. The mild operating temperatures, which do not compromise the stability of the active substance, is very advantageous when compared to other strategies for incorporation of active substances such as thermal extrusion, where the temperatures employed in the film manufacture can exceed 200 ºC [8].

Additionally, there is no requirement to modify the polymer surface in order to improve adhesion properties that promote the impregnation of compounds [16-19].

From an environmental point of view, SSI is considered to be a "green" technique since minimal amounts of polar solvents are required and generally only in cases where the active substances are not well dissolved by the CO_2 [20]. Moreover, solvent-free films are obtained and a final evaporation is usually not required which is advantageous for film integrity. Therefore, SSI is a suitable alternative for the inclusion of an active substance on a polymer matrix after processing. The use of this technique in PET and PP polymers has been previously reported in the literature associated with food, medical and textile fields. For example, Belizón et al. [21] developed a PET/PP multilayer film impregnated with mango extract that was effective in the preservation of lettuce and tangerine. Champeau et al. [22] used polymers such as PP and PET as suture materials that were effectively impregnated with drugs as acetylsalicylic acid or ketoprofen for medical purposes, whereas Herek et al. [23] and Miyazaki et al. [24] used supercritical impregnation for polymer dyeing.

Despite the wide applicability of this technique, one potential disadvantage of SSI is the consequences that the severe operational conditions may have on the integrity of the polymer matrix which can include delamination, the appearance of bubbles, and weakness or loss of mechanical properties. Factors such as the impregnation conditions, the presence of the active compound or the supercritical CO_2 ($scCO_2$) sorption of the polymer can potentially cause damage to the matrix due to the swelling and plasticizing effects directed to the amorphous regions of the polymer [25-27]. This could subsequently alter some chemical and physical characteristics of the films including the morphology, the thermal stability or the mechanical properties [28].

The process of SSI consists of three general steps which can be performed using one or two vessels: (i) solubilisation of the active substance in the supercritical phase; (ii) swelling of the polymer matrix in the supercritical phase; and (iii) diffusion of the active compound into the swollen polymer. Depressurization is then performed which facilitates the impregnation of the active compound into the matrix [29, 30]. The most common method of supercritical impregnation is *via* static or batch mode (BM), although some investigators have started to apply a dynamic or semi-continuous mode (SM) in order to improve impregnation efficiency [29, 31, 32]. In BM, the process proceeds with the vessel's outlet closed and the $scCO_2$ is introduced until the pre-set pressure conditions are reached inside the vessel. In contrast, the SM process involves a stream of $scCO_2$ at a constant pressure that flows across the impregnation cell continuously. In one example, Ivanovic et al. [33] investigated the BM impregnation of thymol in poly(caprolactone) (PCL) and poly(caprolactone-hydroxyapatite) in a single vessel, by placing the polymers in two different baskets with the extract placed at the bottom. Milovanovic et al. [31] used the same procedure but compared the results with those obtained with an integrated process of extraction-deposition of thyme carried out in two vessels with CO_2 recirculation. Furthermore, Manna et al. [34] successfully impregnated poly(vinyl pyrrolidone) microparticles with ketophen using an SM process with two vessels both working at the same conditions of pressure and temperature.

Clearly, a wide range of polymers impregnated with both chemicals and natural extracts using $scCO_2$ have been reported in the literature [35-39]. Among the natural compounds, OLE has been used for food preservation due to its reported AO, antibacterial and antifungal properties [40-44]. Moreover, the olive tree is one of the main crops grown in the Mediterranean basin and is therefore a widely available resource and a by-product of potential interest.

The present paper is aimed at reporting the development of an antioxidant PET/PP laminated film impregnated with OLE by the SM and BM processes carried out in one vessel by investigating the effect of $scCO_2$ flow rate, OLE, and impregnation conditions have over the film properties. To the best of our knowledge, this is the first time that the results obtained by these two impregnation modes have been compared.

2. Material and Methods

2.1. Chemical Reagents and Raw Materials

Carbon dioxide (99.99%) was purchased from Abello-Linde S.A. (Barcelona, Spain). The reagents required for the determination of the antioxidant activity of the impregnated samples, 2,2-diphenyl-1-picrylhydrazyl (DPPH) reagent and ethanol, were supplied by Sigma-Aldrich (Steinheim, Germany).

The polymer film used for impregnation was a multilayer food contact packaging film provided by Technopack Univel S.r.L. (Mortara, Italy). It is comprised of separate layers of PET (12 μm) and PP (50 μm) that are bonded with a urethane adhesive layer. The film thickness specifications were provided by the manufacturer.

Olea europea leaves were collected from the region of Jaén (Andalucía, Spain) and dried at room temperature and stored in darkness prior to extraction of the OLE. The latter was obtained from 200 g of crushed olive leaf, which was placed in a 1 L reactor. Enhanced solvent extraction was carried out over a period of 2 h at 120 bar and 80 ºC using CO_2 and ethanol (1:1) as a co-solvent at a total flow rate of 10 g min^{-1} following the procedure described by Cejudo Bastante et al. [15].

2.2. Supercritical Impregnation Procedures

The supercritical impregnation equipment was supplied by Thar Technologies (Pittsburgh, PA, USA, model SF500), which includes a vessel (500 mL) coupled with a thermostatic jacket, one high pressure pump with a maximum flow rate of 50 g min^{-1}, CO_2 cylinder, and a back-pressure regulator to control system pressure. For both impregnation methods (BM and SM), the equipment layout is the same but the procedure has some differences to the BM procedure reported previously [15]. In both procedures, 1.7 g of plastic film measuring 8 × 30 cm was loaded into the steel supports of the vessel and oriented helically to allow the extract to flow through the layers of the film. Ensuring there was no contact with the film, 15 mL of OLE was loaded in the bottom of the vessel. This amount of OLE was in excess according to a previous study and as such was not considered a limiting factor [15]. During the pressurization step, CO_2 was pumped at a rate of 10 g min^{-1} until the working pressure was achieved. In the BM process, the vessel outlet was closed and when the required pressure was achieved inside, it was maintained for a period of 1 h. An agitation of 40 rpm was applied to enhance mixing and solubilization of the extract in the supercritical phase. For the SM process, a fresh CO_2 stream was continuously introduced at a flow rate of 2 g min^{-1}, flowing outside the system but maintaining the pressure inside the vessel. The CO_2 enters the vessel from the bottom and exits the vessel at the upper side, creating a forced movement of the CO_2 inside the vessel which effectively agitates the agents. Films were submitted to pressures of 100 and 400 bar and temperatures of 35 and 55°C in both impregnation modes. Once the pressure and temperature conditions were achieved in the vessel, impregnation time commenced and after 1 h of impregnation, a controlled depressurization step was carried out at a rate of 100 bar min^{-1}. In order to evaluate the influence of the operational conditions on the film, samples with no extract were also prepared under the same conditions with films treated with CO_2 only tested in BM. All impregnation conditions were carried out in duplicate.

2.3. Determination of the Antioxidant Loading of OLE in the Film

The DPPH assay is widely used as a method for determining the AO activity of natural extracts in the liquid state [45-47] or immobilized in solids [21, 38], as in the case of impregnated matrices. The reduction of the DPPH reagent in the presence of an impregnated film provides a measure of the AO capacity that the film achieved after impregnation. In this sense, the DPPH reaction was used as an indirect measurement for calculating the loading of the AO compounds introduced by the OLE impregnation of the film. Following the procedure described previously [15], 4 mL of 6×10^{-5} M DPPH was placed in contact with a known amount of impregnated film. The decrease of the absorbance at 515 nm was measured after 2 h of incubation at room temperature and in darkness, when a steady state was achieved. The percentage of inhibition (%I), which represents the concentration of compound that reacts with a given amount of DPPH, was calculated using the following equation:

$$\%I = \frac{A_O - A_i}{A_O} \times 100 \qquad (1)$$

where A_0 is the initial DPPH absorbance and A_i is the absorbance after 2 h. The relationship between the concentration of OLE (C (μg/mL)) that reacts with the DPPH after 2 h and I% is given by the following empirical equation:

$$C = -0.0163\ (\%I)^2 + 2.582\ (\%I) + 0.2498 \qquad (R^2 = 0.999) \qquad (2)$$

The AO loading of OLE in the film, expressed in terms of mg AO/g film, was calculated from the value of C determined from Equation (2) and the mass of film used in the reaction.

2.4. Structural Analysis using FTIR

Analyses of film surfaces were performed using a Perkin Elmer Frontier FTIR spectrophotometer (Waltham, USA) fitted with a diamond crystal ATR accessory. Each spectrum of the film surface was the average of 16 scans at a resolution of 4 cm^{-1} over the frequency range 4000–650 cm^{-1}. All spectra were recorded at 25°C and the background spectrum of the clean ATR crystal was collected similarly and automatically subtracted from the sample spectra. Six measurements were performed for each layer of the film, and each condition was measured in duplicate.

2.5. Thermal Analysis using DSC and TGA

A Mettler Toledo DSC1 instrument was used to study the melting endotherms of the films with samples of 4 to 5 mg of film weighed and encapsulated in 30 µL aluminium pans. Using an empty pan as a reference, thermograms were obtained by heating samples from 35 to 300°C, with heating and cooling rates of 10 °C min^{-1} and a 50 mL min^{-1} nitrogen gas flow during the analyses. Single experiments were performed on whole film samples without separating the individual layers and the melting temperature (T_m) and melting enthalpy (ΔH_m) were calculated using STAR^e Evaluation Software (Mettler Toledo, version 11.00). The degree of crystallinity ($\% X_c$) was calculated from the area under the enthalpy of fusion endotherm using the following equation:

$$\% X_c = \frac{\Delta H_m}{\Delta H^0{}_m} \times 100 \qquad (3)$$

where $\Delta H°_m$ is the melting enthalpy of 100% crystalline PET (140 J g^{-1}) or PP (207 J g^{-1}) [48]. The values of ΔH_m are normalized by the DSC software with respect to the total mass of the sample added to the DSC crucible. Since the polymer film is a laminated structure, the values of ΔH_m were corrected to consider the mass fraction of each component relative to the total mass of the sample in order to calculate the $\% X_c$ for each polymer. The correction factor was derived to account for the density (literature values: PET density 1.38 g cm^{-3} [49]; PP density 0.946 g cm^{-3} [50]) and the thickness of each layer (see Section 2.1). For a two-layered laminated film, the mass fraction of component 1:

$$m_1 = \rho_1 \times V_t \qquad (4)$$

where ρ_1 is the density of component 1 and V_t is the total volume of both component layers which is the product of the area and height of the component films and assuming a unit area, the expression becomes:

$$m_t = \rho_1 \times \frac{h_1}{h_1+h_2} \qquad (5)$$

where h_1 and h_2 are the heights of components 1 and 2 respectively. Since the values of densities and thickness are known and constant, the correction factor for the value of ΔH_m for component 1 is given by:

$$\Delta H_{m1} = \Delta H_m / m_t \qquad (6)$$

A Mettler Toledo TGA/DSC1 instrument was employed to perform the TGA experiments. Samples of 4 to 5 mg of film were weighed and placed into 70 µL alumina crucibles prior to heating from 20 to 600 °C at 10°C min^{-1} under a nitrogen atmosphere flow rate of 50 mL min^{-1}. Data were collected with the Mettler STAR^{e} Evaluation software and were then exported to Excel for further processing. The kinetics of thermal decomposition and the apparent activation energy, E_a, were assessed using algorithms described by Bigger et al. [51] .

2.6. Mechanical Property Measurement

The tensile strength (TS), of the impregnated films was measured at 25°C using an Instron Universal Testing Machine model 4301 with a load cell of 5 kN. Six tensile specimens from each sample were prepared by cutting strips measuring 1 × 12 cm. The initial gauge length was set at 100 mm and during the test, a constant cross-head speed of 100 mm min^{-1} was used. The average TS was calculated using Instron BlueHill Series IX software.

2.7. Statistical Analysis

A series of ANOVA tests were carried out to establish statistical differences among the samples. A *post-hoc* Tukey test at $\alpha = 0.05$ was then performed using STATISTICA 8.0 software.

3. Results and Discussion

3.1. Influence of Operational Conditions on Antioxidant Loading of OLE in the Film

Pressure and temperature are the main factors that influence the solvating capacity and diffusivity of $scCO_2$, and the thermodynamic behaviour of the polymer (swelling and plasticizing effects). This work evaluates the effect of pressure and temperature in the range of 100-400 bar and 35-55°C respectively, on the supercritical solvent impregnation of OLE into PET/PP films. In this case, the AO loading of OLE was calculated by analysing the reduction in the absorbance of the DPPH solution in presence of an impregnated film. This reaction indicates the AO capacity of the film, which is determined by the amount of AO compounds from OLE that have been impregnated. The AO loading of the films impregnated by the SM and BM processes under the different conditions is shown in Figure 1, where statistical differences have been analysed by the Tukey test at $\alpha = 0.05$ of significance.

When evaluating the influence of the operational parameters on the loading of impregnated films several factors must be considered including the CO_2-OLE affinity [26] and the OLE-polymer affinity. These are related to the solubility and the partition coefficient, as well as the CO_2-polymer affinity [52] and depend partially on the crystallinity [25] and on the CO_2 sorption capacity of the polymer. These factors are of prime importance when the impregnation process is performed in a single vessel since there is only one set of conditions used for both the solubilisation and impregnation of the active substance. Hence, conditions must be chosen to optimize both the solubilisation of the active substances in the CO_2 and the impregnation efficiency.

Samples impregnated by BM at 400 bar generally showed a significantly higher loading than those impregnated at 100 bar. These results are in agreement with a previous study of the BM impregnation of OLE in PET/PP films, where a high concentration of compounds from different families were impregnated at high pressure [53]. In the case of the dyeing process for PET, several authors agree that higher pressures favour the CO_2 sorption with increasing temperatures [54], which could lead to a better swelling and plasticizing effect and eventually a greater diffusion coefficient [23, 55]. Other authors have also reported higher CO_2 sorption on both PET and PP under increasing pressures at a temperature of 40 ºC [56, 57]. In contrast, previous work on the same matrix showed different results when mango extract was used in a BM process where better impregnation conditions were obtained at 100 bar and 45ºC in a multilayer PET/PP film [21]. This indicates impregnation process depends on the modifications of polymer when it is in contact with the CO_2, but also on the type of active compound, and even more when it is a complex mixture of different compounds such as natural extracts.

When working in SM, the influence of the impregnation conditions differed to those observed in BM where the opposite conditions offered similar AO loading. Since OLE is a mixture of compounds with different polarities, it is possible that applying the 100 bar and 35ºC conditions favoured the impregnation of different compounds than those impregnated at 400 bar and 55ºC, providing similar antioxidant capacity levels in both conditions. Conversely, films impregnated at 100 bar and 55ºC had the lowest AO loadings because these conditions are unfavourable for both the swelling of the polymers and the solubility power of the $scCO_2$/ethanol mixture.

The influence of the impregnation mode is evident when one compares the AO loadings at 400 bar and 35ºC that were obtained under the BM and SM processes. Since the vessel outlet is closed in BM, the optimal conditions of impregnation must favour both solubilisation of the extract and plasticizing of the film in order to achieve the highest level of impregnation. This was not the case for the SM, where the $scCO_2$-OLE affinity would prevail over the OLE-polymer affinity, favouring the drawing or removal of OLE outside the vessel and consequently reducing the film loading. This may explain why films impregnated at 400 bar and 35ºC in BM showed statistically higher AO loadings than those impregnated in SM.

It was evident that although the SM process did not involve a controlled means of agitation within the system, the uniformity of the film loading improved as suggested by the lower standard deviations of the loadings when compared to the BM process. It is possible that the flow of CO_2 in the reactor during the process assists in the homogenization of the $scCO_2$ and OLE thereby enhances the impregnation process.

3.2. Structural Analysis of Films by FTIR

3.2.1. Effect of $scCO_2$ on Non-impregnated Film

The surface structure of each film layer subjected to each of the $scCO_2$ treatments was elucidated by FTIR spectroscopy with the peaks normalized at 2919 cm^{-1} and 1243 cm^{-1} for the PP and PET layers respectively. When compared to the control film with no treatment, the PP layer of the samples subjected to the high-pressure impregnation conditions showed differences at wavenumbers 3430, 3240

(—OH and —NH stretch) and 1646 cm^{-1} (—CH_2=CH_2 stretch) as shown in Figure S2 (supplementary data). These peaks are clearly present in the control film but subsequently diminish upon treatment. They are possibly related to hydroxyl stretching originating from the polyurethane adhesive [58] between the layers. During impregnation, the CO_2 produces a swelling effect which generates mobility of the polymer chains and may subsequently reduce the penetration of the IR beam so that the adhesive is no longer visible. This suggests that the swelling effect may be partially irreversible and/or the ordering of the polymer chains upon depressurization is modified.

In the case of the PET layer, analysis of the samples subjected to scCO_2 treatment did not show any discernible differences (see Figure S1 supplementary data). The observed spectra are almost identical except for a slight decrease and broadening of the peak at 1713 cm^{-1} (–C=O carbonyl stretch and/or –NH-CO-O-R urethane stretch) [59], possibly due to hydrogen bonding, which is evident mostly for samples treated at 55ºC. The extent of the decrease in the peak intensity is not as significant as that observed in the PP layer which may be due to the higher mobility of the polymer chains and the subsequent rearrangement upon depressurization.

Some authors have reported the presence of CO_2 is evidenced by peaks at 2300, 3590 and 3695 cm^{-1} [60, 61] but in the present study, no differences were observed between the control and treated samples at those wavenumbers so it is suggested there is an insignificant amount of CO_2 remaining after the impregnation of the film.

3.2.2. Effect of scCO_2 Impregnation of OLE on Film Structures

Surface FTIR-ATR revealed the presence of functional groups and the possible interactions of these with the film upon the introduction of OLE into the scCO_2 reactor vessel. As shown in Figure 2a, differences in bond vibrations were observed in the PET layer including: hydroxyl vibrations between *ca.* 3000-3650 cm^{-1} [62], symmetric and asymmetric CH_2 and CH stretching vibrations at 2920 and 2851 cm^{-1} [63], >C=O carbonyl stretch and/or urethane stretch –NH-CO—O-R at 1713 cm^{-1} [58, 64, 65], –C-O– stretch of ester groups at 1018 cm^{-1}, para-disubstituted benzene stretching at 872 cm^{-1} [66],

–CH_2 skeletal vibration at 724 cm^{-1} [67], –NH_2 antisymmetric stretching of urethane at 3430 cm^{-1}, and –SO_3H in sulfonic acids at 1280 and 1050 cm^{-1} [59] from the OLE.

Compared with the spectrum of the control film, the intensity of the peaks at 3340, 2920, 2851 cm^{-1} increased in the presence of OLE which can be explained by the glucose and aromatic rings within the structures of the OLE-impregnated phenols [53] and which, in turn, confirms the presence of the OLE on the surface of the impregnated PET layer. Saroufim et al. [68] suggested that the increased absorption band in the region 3340-2850 cm^{-1} is due to the formation of large quantities of polar groups. In the present study, the peaks at 872 and 724 cm^{-1} were also prominent due to the presence of the OLE, although the location and intensity of these peaks did not vary significantly over the operational conditions. It is possible that the OLE is bonded to the film *via* the carbonyl moieties in the OLE, which may explain the decrease in the peak at 1714 cm^{-1} when comparing the impregnated samples with the control film. This result is in agreement with several authors who reported that decreases in this band is due to hydrogen bonding of the carbonyl groups between different compounds and different polymeric matrices including cellulose acetate [69], poly(methyl methacrylate) [70], PVP [34], and contact lens materials [71]. Moreover, the broadening of this peak can also reveal the presence of hydrogen bonding [65], which is favoured when the pressure and temperature are increased during the impregnation process.

Champeau et al. [52] described two mechanisms of impregnation depending on the affinity between the active substance and polymer: (i) impregnation, where the affinity is good and hydrogen bonding takes place; and (ii) deposition, where the affinity is poor or non-existent and the compounds are trapped on the polymer. In the present study, it is possible that impregnation occurs within the PET layer, and thus a strong interaction takes place between the OLE and the polymer that is evidenced by the peak at 1713 cm^{-1}. In the case of the PP layer, which is mostly comprised of long chains of saturated carbon with no functional groups, it is possible that deposition occurs rather than impregnation, and thus a "physical interaction" takes place which does not result in a reduction of the peak intensities of the samples' spectra compared to the control. This has been suggested previously by Kazarian [26], who reported that methyl groups lack the capacity of CO_2 to form interactions with functional groups.

Consequently, the band positions of the OLE in the present study suggest that the apparent new bonds observed on the PP layer are due to the presence of OLE (see Figure 2b). The most intense peak variations are observed in the region of 3500-3000 cm^{-1} which is related to the O-H vibration and $–NH_2$ stretching as previously described, with variations also observed in the range of 1790-1550 cm^{-1}. These results are in agreement with Rojas et al. [72], who reported that the >C=O stretching band at 1715 cm^{-1} resulting from the impregnation of LLDPE with 2-nonanone is a combination of smaller bands: non-associated carbonyl groups bound by dipole interactions (>1680 cm$^{−1}$), or carbonyl groups that are weakly hydrogen bonded to other compounds (1679–1665 cm$^{−1}$) or strongly hydrogen bonded to other compounds (<1664 cm$^{−1}$). Shao et al. [73] related the stretching vibration of the carbonyl group at 1672 cm$^{−1}$ to the benzene ring skeletal vibration at 1625 cm$^{−1}$, which is in the region of the peak vibrations in the present study and this may confirm the presence of the OLE on the film surface. Similarly, the peaks in the region 1455-1355 cm^{-1} which are related to the $-CH_2$ skeletal vibration [74], are observed to increase with respect to the film control, which is also observed in the OLE spectrum.

Comparison of the FTIR spectra obtained at 400 bar in both PP and PET layers showed that there were no observable differences between the impregnation modes along the wavelength range studied (see Figure 2). The spectra of the samples treated at 400 bar and 55ºC in either mode provided the highest relative intensity signals. Conversely, when films were impregnated at 100 bar, the SM spectra signals were slightly increased in both layers compared to those of the BM spectra (Figure S3 and S4). This may be related to the higher AO loading shown previously for the film impregnated at 100 bar and 35ºC by SM.

It can therefore be suggested that the SM process resulted in more significant differences in the FTIR spectra than the BM process and that the higher pressures and temperatures also resulted in greater changes in OLE interactions. In addition, the PP layer was more significantly affected by structural changes than the PET layer. The observed structural modifications are not necessarily related to changes in AO activity since the type of interaction (i.e. impregnation or deposition) can influence the accessibility of the compounds and the subsequent reaction with the DPPH.

3.3. Thermal Analysis

3.3.1. Differential Scanning Calorimetry

All DSC thermograms showed peaks that are typical of PET and PP polymers with the glass transition temperature (T_g), cold crystallization temperature (T_{cc}), and melting temperature of each layer (T_m) observed (see Figures 3A and 3B and Figure S5). The T_g is associated with changes in the amorphous region of polymers which depends on the mobility of the polymer chains; the T_m is determined by the transition of the crystalline regions and is specific to each layer; and the T_{cc} is the transition from amorphous to crystalline states where the molecules may achieve, at a certain stage, freedom of motion enough for ordering themselves spontaneously into a crystalline form [75].

The results of the various transitions obtained from the thermograms are summarized in Table 1 and when compared statistically to the results of the control film ($\alpha = 0.05$), some modifications were observed in the cases of samples treated with scCO_2 without impregnation. Samples processed at 35ºC resulted in reduced crystallinity of the PP with little effect on the crystallinity of the PET layer. Conversely, when samples were processed at 55°C, PP crystallinity was not affected but the T_g of the PET layer was increased. The crystallinity of PET layer remains almost unaffected by the process since the crystalline regions in the polymer do not significantly influence the T_g phenomenon, which is a property associated primarily with the amorphous regions.

Champeau et al. [56] defined two conditions for a polymer to have a high CO_2 sorption: (i) the chain mobility, and (ii) the interactions with CO_2. In the present study, PP and PET only fulfil the condition of low sorption of CO_2. The phenyl groups of PET provide rigidity to the polymer structure and considering that the working temperature remains lower than its T_g, chain mobility is restricted. However, PP has good chain mobility, and the rearrangement of the chains results in a decrease in the crystallinity. Conversely, the phenyl and carbonyl groups of PET can form specific interactions with CO_2 [76], and as the FTIR analysis also revealed in the present study, these interactions could be favoured at 55ºC, which could lead to the observed increase in T_g.

In the case of impregnated samples, differences were found in the crystallinity and T_g of the OLE-impregnated samples which suggests that the presence of the extract may be also responsible for the observed changes in these parameters. As shown in Table 1, when compared to the control film, increasing the pressure lowered the %X_c in the PP layer for both modes of impregnation and for both temperature conditions of CO_2 treatment without OLE. However, the presence of the extract did not substantially affect the PET crystallinity. Since the crystallite size rather than the %X_c influences the melting and glass transition temperatures, the scCO_2 process may have a greater influence on the crystallite size of PP in particular.

At a pressure of 400 bar, a significant reduction in %X_c is observed as a result of the reorganization of the PP polymer chains caused by the CO_2 sorption at which point CO_2-polymer interactions take place [77]. Moreover, PP chain mobility is favoured in the presence of the extract since the use of co-solvent has been reported to enhance the swelling effect in polymers [21, 78] and a decrease in the crystallinity with the incorporation of other compounds has also been reported in PP [79] and other polymers [80-82]. Since the amorphous regions are increased, mass transfer is favoured [54] thereby increasing the level of impregnation. This was also observed in the present study with regard to the extent of loading (see Figure 1). Although the level of impregnation was measured on the whole film rather than on separate layers, higher pressures generally resulted in a higher AO loading.

It was only possible to observe the T_g of the PET layer as the T_g of PP typically occurs at sub-freezing temperatures which are outside the range measurable with the instrument that was used. Generally, supercritical impregnation leads to a decrease in T_g, either due to the swelling effect of CO_2 or the presence of the extract, both of which impart a plasticizing effect [78, 83]. The temperature at which the impregnation process is conducted can therefore have a significant effect on the T_g of the resulting film. In particular, the presence of OLE in samples processed at 55ºC contributed to the increase of T_g values previously observed in samples submitted to the CO_2 conditions. This may be due to the increased hydrogen bonding observed in the FTIR analyses [65] (Figure S1) and that may be at a maximum at the higher temperature, which may confirm the hypothesis of the chemical bond between OLE and PET layer.

3.3.2. Thermogravimetric Analysis

As shown in Figure 4, the thermal degradation of the control PET/PP film, and the films subjected to a BM processes with OLE extract occurred over a single step which is confirmed by a single peak in the first derivative curves (see Figure 4). Moreover, there is no separate step that can be attributed to the OLE extract in the thermogravimetric (TG) profile suggesting that these profiles correspond to the degradation of the polymer alone where the multilayer film is behaving as a homogeneous system. In the typical TG profile of the samples used in the current study, there is a significant mass loss commencing at between 300 and 350ºC which corresponds to degradation of the polymers and, in all cases, no residual inorganic content was observed after 800°C [84].

Kinetic analyses were performed on the thermograms in order to extract the apparent activation energy (E_a) of the degradation step in accordance with the method described by Bigger et al. [51]. The method is based on an iterative computerized technique in which various, well-established models [85-88] are applied to the mass loss curve in order to obtain the best fitting model under the same test conditions and to extract the E_a values. Table 2 shows the results of the TGA fitting analysis and, in general, the fit to the three-dimensional diffusion (D3) and first-order (F1) models are the strongest with the D3 model presenting consistently high R^2 values for the fitting parameter for all samples.

In the D3 model of decomposition, the expression that describes the model with respect to the degree of conversion, α, is given by [88]:

$$g(\alpha) = [1 - (1 - \alpha)^{1/3}]^2 \tag{7}$$

The solution of $g(\alpha)$ is a function of the integral, $p(x)$, and therefore a plot of $g(\alpha)$ *versus* $p(x)$ should give a straight line if the correct model is applied [51]. As shown in Figure 5, a straight line is obtained in the example plot of the sample impregnated by batch mode at 400 bar and 35℃ and the R^2 values associated with the measurement of E_a values in Table 2 are consistently high (i.e. > 0.99). With the exception of the sample prepared by the BM process at 55℃ and 400 bar, there appears to be an overall trend between the OLE loading (Figure 1) in the samples and the E_a with the observed E_a decreasing with increasing OLE loading. This could be due to the thermal destabilizing effect produced by the low levels of OLE or its degradation products (not detected in the TGA profiles) that are present in the polymer matrices of the laminate film. Furthermore, under certain conditions used in the impregnation process the observed average E_a values are higher than the control film.

Table 3 summarises the apparent activation energy values listed in Table 2 in terms of the effects of temperature, pressure and impregnation mode on this parameter. The average apparent E_a values vary from 340 to 385 kJ mol^{-1} with an E_a value of 372 ± 6 kJ mol^{-1} obtained for the control film with no treatment. In general, and with the exception of the sample prepared by the BM process at 35℃ and 400 bar, the upward trend in the observed E_a with increasing $\%X_c$ values (see Tables 1 and 2) for those samples prepared at 35℃ may be related to the increased stability imparted to the polymer by the increased crystallinity. However, there are several components undergoing pyrolysis including PET, PP, PU adhesive, and OLE with the OLE itself a combination of many compounds. As such, there are many competing processes and there was no general trend observed among the E_a values observed as a result of the different treatments (see Table 3). Any trends amongst the different treatments and conditions would require further investigation to be identified.

3.4. Tensile Strength

Table 4 shows the results of the tensile strength (TS) measurements. Samples subjected to $scCO_2$ treatment at 55ºC and either 100 or 400 bar without OLE exhibited higher TS values than those samples processed at 35ºC. This elevation in TS with processing temperature was also observed in the cases of samples containing OLE and subjected to BM processing (see Table 4). Upon the addition of OLE the difference in TS resulting from the processing at 55ºC and the control was reduced but there is still a significant difference with respect to the 35ºC treatment.

The results are consistent with the DSC analyses where the T_g values were observed to be higher for samples impregnated at 55ºC than at 35ºC. This may be due to a hydrogen bonds between PET and OLE which can strengthen the polymer chains and increase the load required to break the polymer film under tension [65] and this is consistent with the findings of the FTIR and DSC analysis. In other systems, the impregnation process has been shown to have little impact on the ductility and mechanical strength of polymer films [89].

The impregnation mode was not a significant variable in any of the structural or thermal analyses with the exception of the mechanical properties. Samples impregnated by the SM process had significantly lower tensile break strength ($\alpha = 0.05$) than those impregnated using the BM process. When comparing samples treated at the same temperature and pressure, the continuous flow of the CO_2 under SM had a significant impact on the tensile strength with lower TS values compared to the BM samples. Although the plasticizing effect of the active compounds loaded into the polymer has been reported to affect the mechanical properties [13], in this case the effect of CO_2 appears to be more dominant than the effect of the extract. There was no apparent relationship between the concentration of the extract and the decrease of the tensile strength. This could be due to the low loading of impregnated compounds or the possibility that the OLE is deposited on the surface only. In any case, it is possible that the technique of tensile testing is insufficiently sensitive to detect the slight differences in the TS that may arise at these low levels of loading. Nevertheless, it is clear that the changes in the mechanical properties are not substantial enough as to compromise their use as packaging material. This is in agreement with the results obtained in the supercritical impregnation of other polymers [77].

4. Conclusions

Supercritical impregnation is a very complex process in which the $scCO_2$-substance-matrix interactions requires optimization of the operational conditions and the method of impregnation. It is clear that the operational conditions will affect polymer films differently depending on their physical and chemical characteristics such as composition, functional groups, thickness and crystallinity. It is therefore critical to evaluate the effect of factors involved in the impregnation processing conditions on key material properties of the film in order to guarantee its integrity after the treatment. In general, the effect of the supercritical treatment was correlated between the FTIR, thermal and mechanical properties analysed. In this study, temperature affected the PP and PET layers differently when CO_2 conditions were applied. Samples treated at 35ºC showed lower PP crystallinity due to the higher chain mobility, whereas samples treated at 55ºC showed increased T_g for the PET due to the reaction of the carbonyl groups with the $scCO_2$ under the respective conditions. The FTIR results of the impregnated samples revealed that impregnation occurred in both layers of the film which is an important factor to consider with regard to film orientation. In the presence of OLE, the influence of $scCO_2$ on the film properties was enhanced, particularly when higher pressures were applied as a result of the favored solubilization of the OLE, the swelling of the PP and the bonding between OLE-PET, thereby favoring the AO loading. Films impregnated at 55ºC subsequently showed higher FTIR signals in both layers and higher T_g values than films subjected only to the CO_2 conditions. Conversely, the decrease in crystallinity of PP was favored at higher pressures when the PP chain mobility chain was increased due to the plasticizing effect of the OLE. The mechanical strength was generally stable for samples treated in BM, with those treated in SM showing lower TS values possibly due to the effect of the continuous CO_2 stream applied during impregnation.

In general, the best impregnation conditions were obtained at 400 bar and 35ºC with a loading rate of 2.5 ± 0.4 mg AO/g film. Under these conditions, there is adequate solubility of the OLE, an increase in the amorphous regions of PP and good interactions between PET and OLE. It is possible that in the samples impregnated at 400 bar and 55ºC, where the conditions of good solubility and higher amorphous regions in PP are also produced, the hydrogen bonding between PET and OLE is such favored such that migration from the PET layer is limited and subsequent reaction with the DPPH reagent are reduced. In this case, the migration of the compounds should be considered in order to ensure that the packaging film will impart adequate food preservation.

The impregnation of natural extracts is also important to optimize given the heterogeneous nature and subsequent solubility of the components. For OLE used in the present study, samples impregnated at 100 bar and 35ºC and 400 bar and 55ºC by SM showed similar AO loadings of 1.8 ± 0.3 and 1.75 ± 0.01 mg AO/g film respectively.

Consideration should therefore be given to the choice of film used for supercritical impregnation only if those changes substantially impact the film properties thereby making it impractical for food packaging purposes. Otherwise, slight modification of the impregnation methods and/or the polymeric substrates may need to be considered in order to obtain effective, active films.

5. Acknowledgments

This work is part of a project granted by the Spanish Government (Project CTQ2014-52427-R) through its financing by the FEDER (European Funds for Regional Development). The authors thank the financial support that University of Cadiz which enabled C.C.B. to perform parts of this study abroad, making this collaboration possible.

6. References

[1] B. Marcos, C. Sárraga, M. Castellari, F. Kappen, G. Schennink, J. Arnau, Development of biodegradable films with antioxidant properties based on polyesters containing α-tocopherol and olive leaf extract for food packaging applications, Food Packag. Shelf Life, 1 (2014) 140-150.
[2] L.J. Lu, L.X. Lu, Preparation and properties of quercetin-incorporated high density polyethylene/low density polyethylene antioxidant multilayer film, Packag. Technol. Sci., 31 (2018) 433-439.
[3] C. Zhou, D. Sun, R. Garcia, F.A. Stevie, Determination of chemical composition in multilayer polymer film using ToF-SIMS,Anal. Methods, 10 (2018) 2444-2449.
[4] C. Colin-Chavez, H. Soto-Valdez, E. Peralta, J. Lizardi-Mendoza, R. Balandran-Quintana, Diffusion of natural astaxanthin from polyethylene active packaging films into a fatty food simulant, Food Res. Int., 54 (2013) 873-880.
[5] N.M. Larocca, R.B. Filho, L.A. Pessan, Influence of layer-by-layer deposition techniques and incorporation of layered double hydroxides (LDH) on the morphology and gas barrier properties of polyelectrolytes multilayer thin films, Surf. Coat. Tech., 349 (2018) 1-12.
[6] A. Cherpinski, S. Torres-Giner, L. Cabedo, J.A. Méndez, J.M. Lagaron, Multilayer structures based on annealed electrospun biopolymer coatings of interest in water and aroma barrier fiber-based food packaging applications, J. Appl. Polym. Sci., 135 (2018).
[7] X. Zhu, K. Schaich, X. Chen, K. Yam, Antioxidant effects of sesamol released from polymeric films on lipid oxidation in linoleic acid and oat cereal, Packag. Technol. Sci., 26 (2013) 31-38.
[8] A. Apicella, P. Scarfato, L. Di Maio, L. Incarnato, Transport properties of multilayer active PET films with different layers configuration,React. Funct. Polym., 127 (2018) 29-37.
[9] E. Joo, Y. Chang, I. Choi, S.B. Lee, D.H. Kim, Y.J. Choi, C.S. Yoon, J. Han, Whey protein-coated high oxygen barrier multilayer films using surface pretreated PET substrate, Food Hydrocoll., 80 (2018) 1-7.
[10] S. Ishtiaque, S. Naz, J. Ahmed, A. Faruqui, Barrier properties analysis of polyethylene terephthalate films (PET) coated with natural Polyphenolic and Gelatin mixture (PGM), Defect and Diffusion Forum, 382 DDF (2018) 38-43.
[11] L. Di Maio, F. Marra, T.F. Bedane, L. Incarnato, S. Saguy, Oxygen transfer in co-extruded multilayer active films for food packaging, AIChE Journal, 63 (2017) 5215-5221.
[12] H.J. Jo, K.M. Park, J.H. Na, S.C. Min, K.H. Park, P.S. Chang, J. Han, Development of anti-insect food packaging film containing a polyvinyl alcohol and cinnamon oil emulsion at a pilot plant scale, J. Stored Prod. Res., 61 (2015) 114-118.
[13] J.P. Cerisuelo, R. Gavara, P. Hernández-Muñoz, Natural antimicrobial - Containing EVOH coatings on PP and PET films: Functional and active property characterization, Packag. Technol. Sci., 27 (2014) 901-920.
[14] M.J. Cocero, Á. Martín, F. Mattea, S. Varona, Encapsulation and co-precipitation processes with supercritical fluids: Fundamentals and applications, J. Supercrit. Fluids, 47 (2009) 546-555.
[15] C. Cejudo Bastante, L. Casas Cardoso, C. Mantell Serrano, E.J. Martínez de la Ossa, Supercritical impregnation of food packaging films to provide antioxidant properties, J. Supercrit. Fluids, 128 (2017) 200-207.
[16] M. Mulla, J. Ahmed, H. Al-Attar, E. Castro-Aguirre, Y.A. Arfat, R. Auras, Antimicrobial efficacy of clove essential oil infused into chemically modified LLDPE film for chicken meat packaging, Food Control, 73 (2017) 663-671.

[17] K. Simonović, I. Petronijević, D. Kostoski, J. Dojčilović, A.S. Luyt, D. Dudić, Effects of acid treatment at different temperatures on the surface dielectric properties of low-density polyethylene, Polym. Int., 63 (2014) 1924-1929.

[18] I. Novák, M. Števiar, A. Popelka, I. Chodák, J. Mosnáček, M. Špírková, I. Janigová, A. Kleinová, J. Sedliačik, M. Šlouf, Surface modification of polyethylene by diffuse barrier discharge plasma, Polym. Eng. Sci., 53 (2013) 516-523.

[19] M.R. Sanchis, V. Blanes, M. Blanes, D. Garcia, R. Balart, Surface modification of low density polyethylene (LDPE) film by low pressure O_2 plasma treatment, Eur. Polym. J., 42 (2006) 1558-1568.

[20] Y. Zhao, K. Jung, Y. Shimoyama, Y. Shimogaki, T. Momose, Kinetic effects of methanol addition on supercritical fluid deposition of TiO_2, J. Supercrit. Fluids, 138 (2018) 63-72.

[21] M. Belizón, M.T. Fernández-Ponce, L. Casas, C. Mantell, E.J. Martínez de la Ossa-Fernández, Supercritical impregnation of antioxidant mango polyphenols into a multilayer PET/PP food-grade film, J. CO_2 Util., 25 (2018) 56-67.

[22] M. Champeau, J.M. Thomassin, T. Tassaing, C. Jerome, Drug Loading of Sutures by Supercritical CO_2 Impregnation: Effect of Polymer/Drug Interactions and Thermal Transitions, Macromol. Mater. Eng, 300 (2015) 596-610.

[23] L.C.S. Herek, R.C. Oliveira, A.F. Rubira, N. Pinheiro, Impregnation of pet films and PHB granules with curcumin in supercritical CO_2, Braz. J. Chem. Eng., 23 (2006) 227-234.

[24] K. Miyazaki, I. Tabata, T. Hori, Effects of molecular structure on dyeing performance and colour fastness of yellow dyestuffs applied to polypropylene fibres in supercritical carbon dioxide, Color. Technol., 128 (2012) 51-59.

[25] D. Sun, R. Zhang, Z. Liu, Y. Huang, Y. Wang, J. He, B. Han, G. Yang, Polypropylene/Silica Nanocomposites Prepared by in-Situ Sol−Gel Reaction with the Aid of CO2, Macromol., 38 (2005) 5617-5624.

[26] S.G. Kazarian, Polymer processing with supercritical fluids, Polym. Sci. - Series C, 42 (2000) 78-101.

[27] E. Kiran, Supercritical fluids and polymers – The year in review – 2014, J. Supercrit. Fluids, 110 (2016) 126-153.

[28] Y. Kong, J.N. Hay, The measurement of the crystallinity of polymers by DSC, Polym., 43 (2002) 3873-3878.

[29] A. Bouledjouidja, Y. Masmoudi, M. Van Speybroeck, L. Schueller, E. Badens, Impregnation of Fenofibrate on mesoporous silica using supercritical carbon dioxide, Int. J. Pharm, 499 (2016) 1-9.

[30] X.-K. Li, H. Lu, G.-P. Cao, Y.-H. Qian, L.-H. Chen, R.-H. Zhang, H.-L. Liu, Y.-H. Shi, Experimental Study of the Synergistic Plasticizing Effect of Carbon Dioxide and Ibuprofen on the Glass Transition Temperature of Poly(methyl methacrylate), Ind. Eng. Chem. Res., 53 (2014) 5873-5885.

[31] S. Milovanovic, G. Hollermann, C. Errenst, J. Pajnik, S. Frerich, S. Kroll, K. Rezwan, J. Ivanovic, Supercritical CO2 impregnation of PLA/PCL films with natural substances for bacterial growth control in food packaging, Food Res. Int., 107 (2018) 486-495.

[32] M.A. Fanovich, J. Ivanovic, D. Misic, M.V. Alvarez, P. Jaeger, I. Zizovic, R. Eggers, Development of polycaprolactone scaffold with antibacterial activity by an integrated supercritical extraction and impregnation process, J. Supercrit. Fluids, 78 (2013) 42-53.

[33] J. Ivanovic, S. Knauer, A. Fanovich, S. Milovanovic, M. Stamenic, P. Jaeger, I. Zizovic, R. Eggers, Supercritical CO2 sorption kinetics and thymol impregnation of PCL and PCL-HA, J. Supercrit. Fluids, 107 (2016) 486-498.

[34] L. Manna, M. Banchero, D. Sola, A. Ferri, S. Ronchetti, S. Sicardi, Impregnation of PVP microparticles with ketoprofen in the presence of supercritical CO2, J. Supercrit. Fluids, 42 (2007) 378-384.

[35] M.L. Goñi, N.A. Gañán, R.E. Martini, A.E. Andreatta, Carvone-loaded LDPE films for active packaging: Effect of supercritical CO2-assisted impregnation on loading, mechanical and transport properties of the films, J. Supercrit. Fluids, 133 (2018) 278-290.

[36] A.M.A. Dias, A. Rey-Rico, R.A. Oliveira, S. Marceneiro, C. Alvarez-Lorenzo, A. Concheiro, R.N.C. Júnior, M.E.M. Braga, H.C. de Sousa, Wound dressings loaded with an anti-inflammatory jucá (Libidibia ferrea) extract using supercritical carbon dioxide technology, J. Supercrit. Fluids, 74 (2013) 34-45.

[37] C.V. da Silva, V.J. Pereira, G.M.N. Costa, E.C.M. Cabral-Albuquerque, S.A.B. Vieira de Melo, H.C. de Sousa, A.M.A. Dias, M.E.M. Braga, Supercritical solvent impregnation/deposition of spilanthol-enriched extracts into a commercial collagen/cellulose-based wound dressing, J. Supercrit. Fluids, 133 (2018) 503-511.
[38] J. Sanchez-Sanchez, M.T. Fernández-Ponce, L. Casas, C. Mantell, E.J.M. de la Ossa, Impregnation of mango leaf extract into a polyester textile using supercritical carbon dioxide, J. Supercrit. Fluids, 128 (2017) 208-217.
[39] C. Sharma, R. Dhiman, N. Rokana, H. Panwar, Nanotechnology: An Untapped Resource for Food Packaging, Front. Microbiol., 8 (2017) 1735.
[40] G. Amaro-Blanco, J. Delgado-Adámez, M.J. Martín, R. Ramírez, Active packaging using an olive leaf extract and high pressure processing for the preservation of sliced dry-cured shoulders from Iberian pigs, Innov. Food Sci. Emerg. Technol., 45 (2018) 1-9.
[41] M. Moudache, C. Nerín, M. Colon, F. Zaidi, Antioxidant effect of an innovative active plastic film containing olive leaves extract on fresh pork meat and its evaluation by Raman spectroscopy, Food Chem., 229 (2017) 98-103.
[42] A. Mohammadi, S.M. Jafari, A.F. Esfanjani, S. Akhavan, Application of nano-encapsulated olive leaf extract in controlling the oxidative stability of soybean oil, Food Chem., 190 (2016) 513-519.
[43] S. Souilem, I. Fki, I. Kobayashi, N. Khalid, M.A. Neves, H. Isoda, S. Sayadi, M. Nakajima, Emerging Technologies for Recovery of Value-Added Components from Olive Leaves and Their Applications in Food/Feed Industries, Food Bioprocess Tech., 10 (2017) 229-248.
[44] M. Herrero, T.N. Temirzoda, A. Segura-Carretero, R. Quirantes, M. Plaza, E. Ibañez, New possibilities for the valorization of olive oil by-products, J. Chromatogr. A, 1218 (2011) 7511-7520.
[45] M.T. Fernández-Ponce, L. Casas, C. Mantell, E. Martínez de la Ossa, Use of high pressure techniques to produce Mangifera indica L. leaf extracts enriched in potent antioxidant phenolic compounds, Innov. Food Sci. Emerg. Technol, 29 (2015) 94-106.
[46] C. Chinnarasu, A. Montes, M.T. Fernandez-Ponce, L. Casas, C. Mantell, C. Pereyra, E.J.M. de la Ossa, S. Pattabhi, Natural antioxidant fine particles recovery from Eucalyptus globulus leaves using supercritical carbon dioxide assisted processes, J. Supercrit. Fluids, 101 (2015) 161-169.
[47] M. Otero-Pareja, L. Casas, M. Fernández-Ponce, C. Mantell, E. Ossa, Green Extraction of Antioxidants from Different Varieties of Red Grape Pomace, Molecules, 20 (2015) 9686.
[48] R.L. Blaine, "Thermal Applications Note, Polymer Heats of Fusion", Technical Note TN048, www.tainstruments.com/pdf/literature/TN048.pdf, accessed April, 2017, (2017).
[49] A. Pawlak, M. Pluta, J. Morawiec, A. Galeski, M. Pracella, Characterization of scrap poly(ethylene terephthalate), Eur. Polym. J., 36 (2000) 1875-1884.
[50] D.C. Bassett, R.H. Olley, On the lamellar morphology of isotactic polypropylene spherulites, Polym., 25 (1984) 935-943.
[51] S.W. Bigger, M.J. Cran, I.S.M.A. Tawakkal, Two novel algorithms for the thermogravimetric assessment of polymer degradation under non-isothermal conditions, Polym. Test., 43 (2015) 139-146.
[52] M. Champeau, J.M. Thomassin, T. Tassaing, C. Jérôme, Drug loading of polymer implants by supercritical CO_2; assisted impregnation: A review, J. Control. Release, 209 (2015) 248-259.
[53] C. Cejudo Bastante, L. Casas Cardoso, M.T. Fernández Ponce, C. Mantell Serrano, E.J. Martínez de la Ossa-Fernández, Characterization of olive leaf extract polyphenols loaded by supercritical solvent impregnation into PET/PP food packaging films, J. Supercrit. Fluids, 140 (2018) 196-206.
[54] J. von Schnitzler, R. Eggers, Mass transfer in polymers in a supercritical CO_2-atmosphere, J. Supercrit. Fluids, 16 (1999) 81-92.
[55] W.L.F. Santos, M.F. Porto, E.C. Muniz, L. Olenka, M.L. Baessso, A.C. Bento, A.F. Rubira, Poly(ethylene terephtalate) films modified with N,N-dimethylacrylamide: Incorporation of disperse dye, J. Appl. Polym. Sci., 77 (2000) 269-282.
[56] M. Champeau, J.M. Thomassin, C. Jérôme, T. Tassaing, In situ FTIR micro-spectroscopy to investigate polymeric fibers under supercritical carbon dioxide: CO_2 sorption and swelling measurements, J. Supercrit. Fluids, 90 (2014) 44-52.
[57] Z. Lei, H. Ohyabu, Y. Sato, H. Inomata, R.L. Smith Jr, Solubility, swelling degree and crystallinity of carbon dioxide-polypropylene system, J. Supercrit. Fluids, 40 (2007) 452-461.

[58] L. Xie, L. Wei, L. Zhiqing, W. Xiaolin, G. Heling, W. Rongjie, G. Xuhong, L. Cuihua, J. Xin, Underwater polyurethane adhesive with enhanced cohesion by postcrosslinking of glycerol monomethacrylate, J. Appl. Polym. Sci., 135 (2018) 46579.

[59] H.F. Shurvell, J.M. Chalmers, Spectra– Structure Correlations in the Mid- and Far- Infrared, in: J.M. Chalmers, P.R. Griffith (Eds.) Handbook of Vibrational Spectroscopy, Wiley, 2006.

[60] M. Champeau, J.M. Thomassin, C. Jerome, T. Tassaing, In situ investigation of supercritical CO_2 assisted impregnation of drugs into a polymer by high pressure FTIR micro-spectroscopy, Analyst, 140 (2015) 869-879.

[61] P.W. Labuschagne, M.J. John, R.E. Sadiku, Investigation of the degree of homogeneity and hydrogen bonding in PEG/PVP blends prepared in supercritical CO_2: Comparison with ethanol-cast blends and physical mixtures, J. Supercrit. Fluids, 54 (2010) 81-88.

[62] R. Abdollahi, M.T. Taghizadeh, S. Savani, Thermal and mechanical properties of graphene oxide nanocomposite hydrogel based on poly (acrylic acid) grafted onto amylose, Polym. Degrad. Stab., 147 (2018) 151-158.

[63] S. Zhang, R. Li, D. Huang, X. Ren, T.-S. Huang, Antibacterial modification of PET with quaternary ammonium salt and silver particles via electron-beam irradiation, Mater. Sci. Eng. C, 85 (2018) 123-129.

[64] I.V. Korolkov, Y.G. Gorin, A.B. Yeszhanov, A.L. Kozlovskiy, M.V. Zdorovets, Preparation of PET track-etched membranes for membrane distillation by photo-induced graft polymerization, Mater. Chem. Phys., 205 (2018) 55-63.

[65] C. Cazan, M. Cosnita, A. Duta, Effect of PET functionalization in composites of rubber–PET–HDPE type, Arab. J. Chem. , 10 (2017) 300-312.

[66] M.M. Lubna, K.S. Salem, M. Sarker, M.A. Khan, Modification of Thermo-Mechanical Properties of Recycled PET by Vinyl Acetate (VAc) Monomer Grafting Using Gamma Irradiation, J. Polym. Environ. , 26 (2018) 83-90.

[67] F.M. Abdul Aziz, S.N. Surip, N.N. Bonnia, K.A. Sekak, The effect of Pineapple Leaf Fiber (PALF) incorporation into Polyethylene Terephthalate (PET) on FTIR, morphology and wetting properties, in: IOP Conference Series: Earth and Environmental Science, 2018.

[68] E. Saroufim, C. Celauro, M.C. Mistretta, A simple interpretation of the effect of the polymer type on the properties of PMBs for road paving applications, Constr. Build Mater., 158 (2018) 114-123.

[69] S. Milovanovic, D. Markovic, K. Aksentijevic, D.B. Stojanovic, J. Ivanovic, I. Zizovic, Application of cellulose acetate for controlled release of thymol, Carbohydr. Polym., 147 (2016) 344-353.

[70] A. López-Periago, A. Argemí, J.M. Andanson, V. Fernández, C.A. García-González, S.G. Kazarian, J. Saurina, C. Domingo, Impregnation of a biocompatible polymer aided by supercritical CO2: Evaluation of drug stability and drug–matrix interactions, J. Supercrit. Fluids, 48 (2009) 56-63.

[71] F. Yañez, L. Martikainen, M.E.M. Braga, C. Alvarez-Lorenzo, A. Concheiro, C.M.M. Duarte, M.H. Gil, H.C. de Sousa, Supercritical fluid-assisted preparation of imprinted contact lenses for drug delivery, Acta Biomater., 7 (2011) 1019-1030.

[72] A. Rojas, D. Cerro, A. Torres, M.J. Galotto, A. Guarda, J. Romero, Supercritical impregnation and kinetic release of 2-nonanone in LLDPE films used for active food packaging, J. Supercrit. Fluids, 104 (2015) 76-84.

[73] P. Shao, Z. Yan, H. Chen, J. Xiao, Electrospun poly(vinyl alcohol)/permutite fibrous film loaded with cinnamaldehyde for active food packaging, J. Appl. Polym. Sci., 135 (2018).

[74] F. López-Saucedo, G.G. Flores-Rojas, J. López-Saucedo, B. Magariños, C. Alvarez-Lorenzo, A. Concheiro, E. Bucio, Antimicrobial silver-loaded polypropylene sutures modified by radiation-grafting, Eur. Polym. J., (2018).

[75] S. Molinaro, M. Cruz Romero, M. Boaro, A. Sensidoni, C. Lagazio, M. Morris, J. Kerry, Effect of nanoclay-type and PLA optical purity on the characteristics of PLA-based nanocomposite films, J. Food Eng., 117 (2013) 113-123.

[76] S.G. Kazarian, M.F. Vincent, F.V. Bright, C.L. Liotta, C.A. Eckert, Specific Intermolecular Interaction of Carbon Dioxide with Polymers, J. Am. Chem. Soc., 118 (1996) 1729-1736.

[77] M.L. Goñi, N.A. Gañán, M.C. Strumia, R.E. Martini, Eugenol-loaded LLDPE films with antioxidant activity by supercritical carbon dioxide impregnation, J. Supercrit. Fluids, 111 (2016) 28-35.

[78] Z. Shen, G.S. Huvard, C.S. Warriner, M. Mc Hugh, J.L. Banyasz, M.K. Mishra, CO2-assisted fiber impregnation, Polym., 49 (2008) 1579-1586.

[79] D.K. Mandal, H. Bhunia, P.K. Bajpai, A. Kumar, G. Madhu, G.B. Nando, Biodegradation of Pro-oxidant Filled Polypropylene Films and Evaluation of the Ecotoxicological Impact, J. Polym. Environ. , 26 (2018) 1061-1071.

[80] A. Torres, E. Ilabaca, A. Rojas, F. Rodríguez, M.J. Galotto, A. Guarda, C. Villegas, J. Romero, Effect of processing conditions on the physical, chemical and transport properties of polylactic acid films containing thymol incorporated by supercritical impregnation, Eur. Polym. J., 89 (2017) 195-210.

[81] S.A. Mir, M.A. Shah, B.N. Dar, A.A. Wani, S.A. Ganai, J. Nishad, Supercritical Impregnation of Active Components into Polymers for Food Packaging Applications, Food Bioprocess Tech., 10 (2017) 1749-1754.

[82] C. Villegas, A. Torres, M. Rios, A. Rojas, J. Romero, C.L. de Dicastillo, X. Valenzuela, M.J. Galotto, A. Guarda, Supercritical impregnation of cinnamaldehyde into polylactic acid as a route to develop antibacterial food packaging materials, Food Res. Int., 99 (2017) 650-659.

[83] M. Jamshidian, E.A. Tehrany, M. Imran, M.J. Akhtar, F. Cleymand, S. Desobry, Structural, mechanical and barrier properties of active PLA–antioxidant films, J. Food Eng., 110 (2012) 380-389.

[84] M.P. Sepe, Thermal Analysis of Polymers, Rapra Technology Limited, 1997.

[85] D. Dollimore, Thermodynamic, kinetic and surface texture factors in the production of active solids by thermal decomposition, J. Therm. Anal., 38 (1992) 111-130.

[86] D. Dollimore, T.A. Evans, Y.F. Lee, G.P. Pee, F.W. Wilburn, The significance of the onset and final temperatures in the kinetic analysis of TG curves, Thermochim. Acta, 196 (1992) 255-265.

[87] D. Dollimore, T.A. Evans, Y.F. Lee, F.W. Wilburn, Correlation between the shape of a TG/DTG curve and the form of the kinetic mechanism which is applying, Thermochim. Acta, 198 (1992) 249-257.

[88] D. Dollimore, The application of thermal analysis in studying the thermal decomposition of solids, Thermochim. Acta, 203 (1992) 7-23.

[89] M.L. Goñi, N.A. Gañán, S.E. Barbosa, M.C. Strumia, R.E. Martini, Supercritical CO_2-assisted impregnation of LDPE/sepiolite nanocomposite films with insecticidal terpene ketones: Impregnation yield, crystallinity and mechanical properties assessment, J. Supercrit. Fluids, 130 (2017) 337-346.

Table 1. Values of T_m, %X_c, T_g, and T_{cc} obtained from DSC thermograms of control (untreated) PET/PP laminate films, films treated with CO_2 and impregnated films with OLE.

		PP		**PET**			
Mode	**Sample**	**T_m/℃**	**%X_c**	**T_g /℃**	**T_{cc}/℃**	**T_m/℃**	**%X_c**
	Control	161.60 ± 0.59	35.95 ± 0.32	82.70 ± 0.28	223.23 ± 5.07	253.30 ± 0.23	29.59 ± 0.47
No Extract (BM)	100 bar, 35℃	161.72 ± 0.11	31.02 ± 1.70	82.20 ± 0.42	227.21 ± 0.64	253.33 ± 0.02	28.81 ± 1.08
	400 bar, 35℃	161.85 ± 0.23	30.93 ± 2.93	82.85 ± 0.49	225.71 ± 1.41	253.14 ± 0.19	30.96 ± 2.97
	100 bar, 55℃	161.12 ± 0.08	35.37 ± 1.42	90.08 ± 1.24	223.75 ± 0.85	253.31 ± 0.43	29.66 ± 1.47
	400 bar, 55℃	161.46 ± 0.09	36.26 ± 1.72	93.63 ± 7.81	222.15 ± 2.84	253.24 ± 0.38	28.68 ± 0.21
BM	100 bar, 35℃	160.60 ± 0.93	35.12 ± 1.13	82.85 ± 0.07	231.18 ± 0.99	253.07 ± 0.15	26.55 ± 3.28
	400 bar, 35℃	163.03 ± 0.87	28.85 ± 1.26	83.06 ± 0.93	233.11 ± 1.70	254.13 ± 0.24	29.16 ± 3.69
	100 bar, 55℃	160.87 ± 0.47	35.25 ± 1.70	96.39 ± 1.85	230.41 ± 4.59	252.64 ± 0.73	29.34 ± 0.79
	400 bar, 55℃	161.78 ± 1.01	33.57 ± 3.04	97.30 ± 1.27	220.97 ± 2.53	252.46 ± 0.76	31.14 ± 2.25
SM	100 bar, 35℃	161.38 ± 0.26	30.58 ± 4.39	102.45 ± 3.32	228.50 ± 1.45	253.31 ± 0.43	28.72 ± 6.16
	400 bar, 35℃	162.19 ± 0.70	30.15 ± 1.74	83.28 ± 0.33	229.75 ± 1.27	253.96 ± 0.43	25.50 ± 2.61
	100 bar, 55℃	161.56 ± 0.79	32.66 ± 2.54	95.22 ± 3.27	227.71 ± 4.61	252.73 ± 0.17	30.63 ± 1.55
	400 bar, 55℃	161.98 ± 0.35	31.61 ± 1.29	86.75 ± 0.07	222.51 ± 0.22	253.08 ± 0.11	27.93 ± 2.14

Table 2. Values of the kinetic model fitting parameter, ρ, linear regression coefficient, R^2, and apparent activation energies, E_a, for the thermal decomposition of PET/PP laminate films subjected to scCO_2 impregnation with and without OLE and under BM or SM conditions (degree of conversion range: $0.1 \leq \alpha \leq 0.9$).

	Control	**No extract (BM)**				**SM**				**BM**			
Kinetic Model		100 bar 35°C	100 bar 55°C	400 bar 35°C	400 bar 55°C	100 bar 35°C	100 bar 55°C	400 bar 35°C	400 bar 55°C	100 bar 35°C	100 bar 55°C	400 bar 35°C	400 bar 55°C
Acceleratory													
Pn Power law	0	0	0	0	0	0	0.001	0	0	0.006	0	0	0
E1 Exponential law	0.517	0.516	0.517	0.516	0.518	0.518	0.518	0.516	0.516	0.518	0.518	0.519	0.516
Sigmoidal													
A2 Avrami-Erofeev	0.781	0.713	0.740	0.730	0.775	0.683	0.736	0.706	0.686	0.733	0.733	0.775	0.714
A3 Avrami-Erofeev	0.760	0.693	0.704	0.710	0.742	0.649	0716	0.687	0.651	0.711	0.707	0.745	0.686
A4 Avrami-Erofeev	0	0	0	0	0	0	0	0	0	0	0	0	0
B1 Prout-Tompkins	0	0	0	0	0	0	0	0	0	0	0	0	0
Deceleratory													
Geometrical													
R2 Contracting area	0.829	0.795	0.814	0.800	0.844	0.808	0.880	0.820	0.767	0.876	0.855	0.854	0.817
R3 Contracting volume	0.873	0.873	0.893	0.864	0.895	0.856	0.872	0.872	0.866	0.874	0.891	0.900	0.889
Diffusion													
D1 One dimensional	0.597	0.545	0.567	0.556	0.609	0.621	0.671	0.575	0.506	0.659	0.610	0.618	0.566
D2 Two dimensional	0.930	0.936	0.940	0.934	0.938	0.960	0.984	0.958	0.936	0.981	0.961	0.943	0.954
D3 Three dimensional	**0.986**	**0.995**	**0.998**	**0.980**	**0.984**	**0.945**	**0.955**	**0.982**	**0.959**	**0.959**	**0.982**	**0.987**	**0.991**
D4 Ginstling-Brounshtein	0.947	0.959	0.962	0.956	0.957	0.956	0.976	0.982	0.958	0.984	0.978	0.960	0.977
Reaction Order													
F1 First order	0.989	0.958	0.976	0.970	0.995	0.908	0.919	0.944	0.961	0.923	0.949	0.973	0.958
F2 Second order	0.889	0.862	0.871	0.874	0.877	0.784	0.798	0.835	0.864	0.803	0.836	0.868	0.848
F3 Third order	0.655	0.639	0.649	0.648	0.643	0.540	0.538	0.603	0.656	0.547	0.597	0.631	0.621
D3 model E_a/kJ mol^{-1}	372 ± 6.1	370 ± 9.6	353 ± 0.2	348 ± 3.3	340 ± 0.6	355 ± 4.8	382 ± 0.2	378 ± 2.6	352 ± 1.2	379 ± 0.4	385 ± 0.4	358 ± 1.0	385 ± 1.1
g(α) vs. p(x) R^2	0.9999	0.9982	0.9999	0.9996	0.9982	0.9995	0.9996	0.9991	0.9987	0.9937	0.9987	0.9998	0.999

Table 3. Average values of apparent activation energies, E_a, for the thermal decomposition of PET/PP laminate films subjected to different treatments. The control is the untreated film.

Treatment		**Average E_a value/kJ mol^{-1}**
Control		372 ± 6.1
Temperature		
	35°C	365 ± 3.6
	55°C	366 ± 0.6
Pressure		
	100 bar	371 ± 2.6
	400 bar	360 ± 1.6
Mode		
	SM	367 ± 2.2
	BM	377 ± 0.7
	No OLE (BM)	353 ± 3.4

Table 4. Tensile strength results of control and impregnated PET/PP laminate films subjected to different treatments.

Mode	Sample	Tensile Strength/kN
	Control	56.5 ± 8
No extract (BM)	100 bar, 35°C	55.4 ± 3.0
	400 bar, 35°C	52.4 ± 4.2
	100 bar, 55°C	62.5 ± 3.1
	400 bar, 55°C	61.5 ± 1.3
BM	100 bar, 35°C	57.1 ± 1.1
	400 bar, 35°C	59.6 ± 2.3
	100 bar, 55°C	65.3 ± 3.9
	400 bar, 55°C	66.5 ± 8.2
SM	100 bar, 35°C	48.6 ± 2.5
	400 bar, 35°C	48.6 ± 4.2
	100 bar, 55°C	54.5 ± 4.9
	400 bar, 55°C	54.3 ± 4.4

*Films treated with CO_2 (no extract) were processed by BM

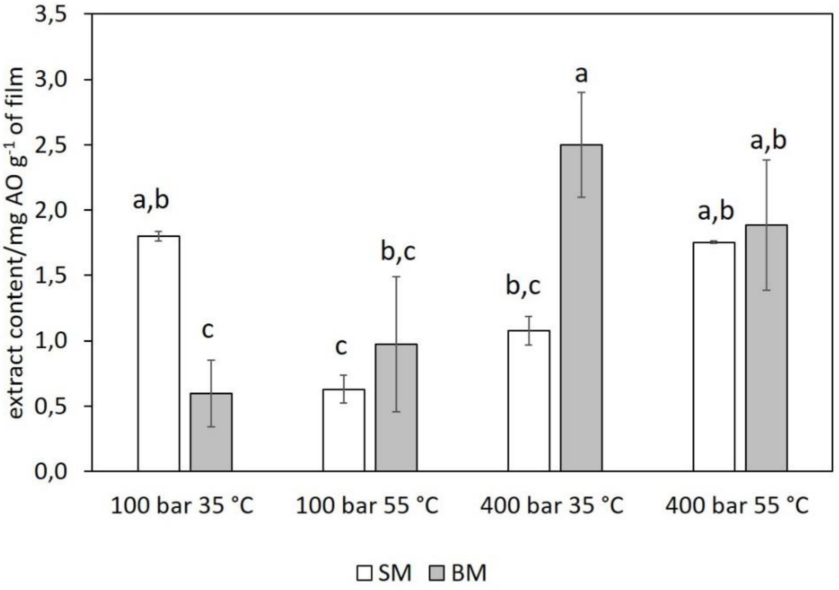

Figure 1. Antioxidant loading in PET/PP laminate films impregnated by the SM and BM processes (n = 3). Letters show statistical differences among samples (α = 0.05).

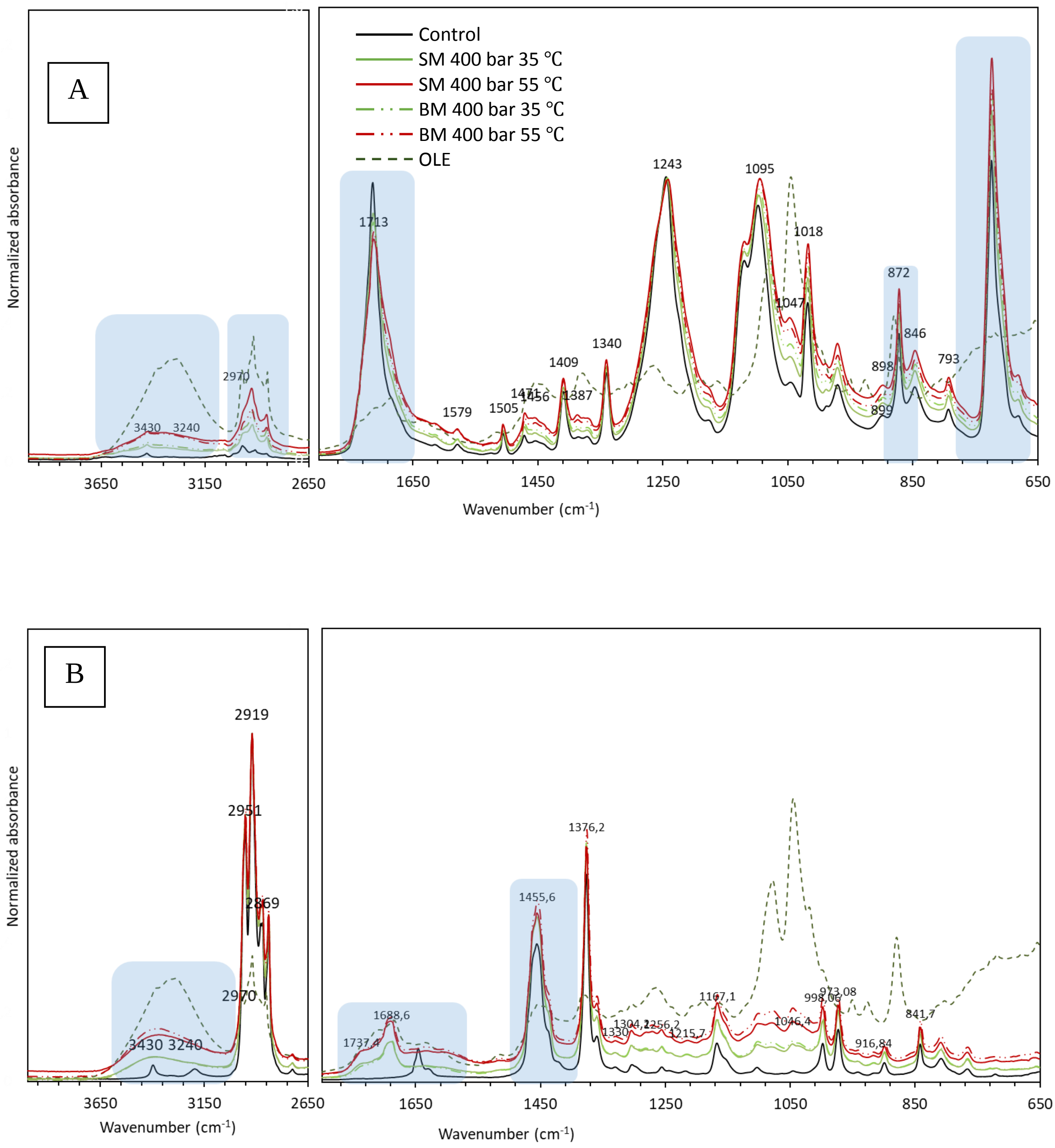

Figure 2. FTIR-ATR spectra of PET/PP laminate film impregnated with OLE at 400 bar: (A) PET layer and (B) PP layer.

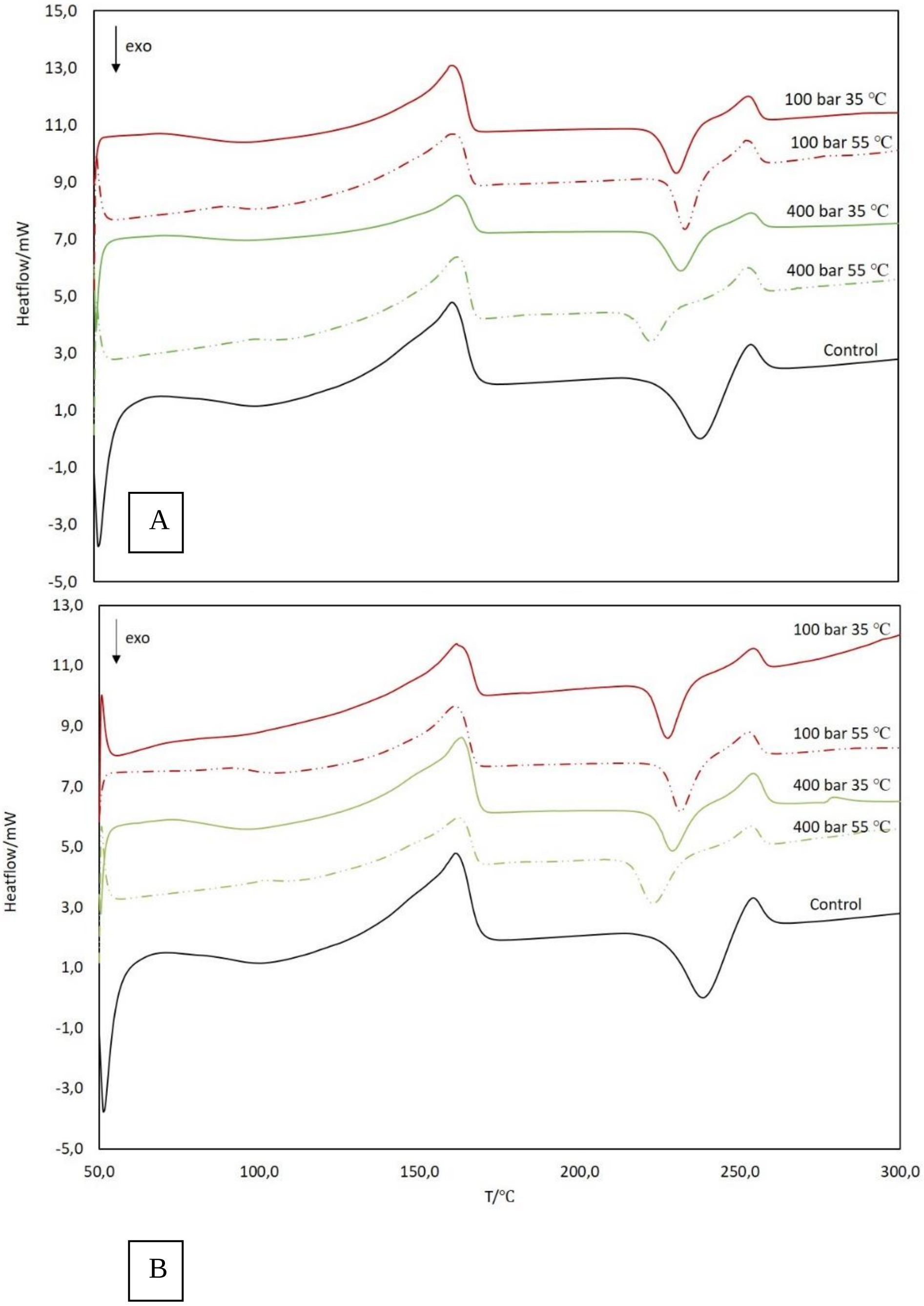

* The control sample is referred to the non-treated film

Figure 3. DSC thermograms of PET/PP laminate film samples impregnated by: (A) SM and (B) BM. The control sample is non-treated film.

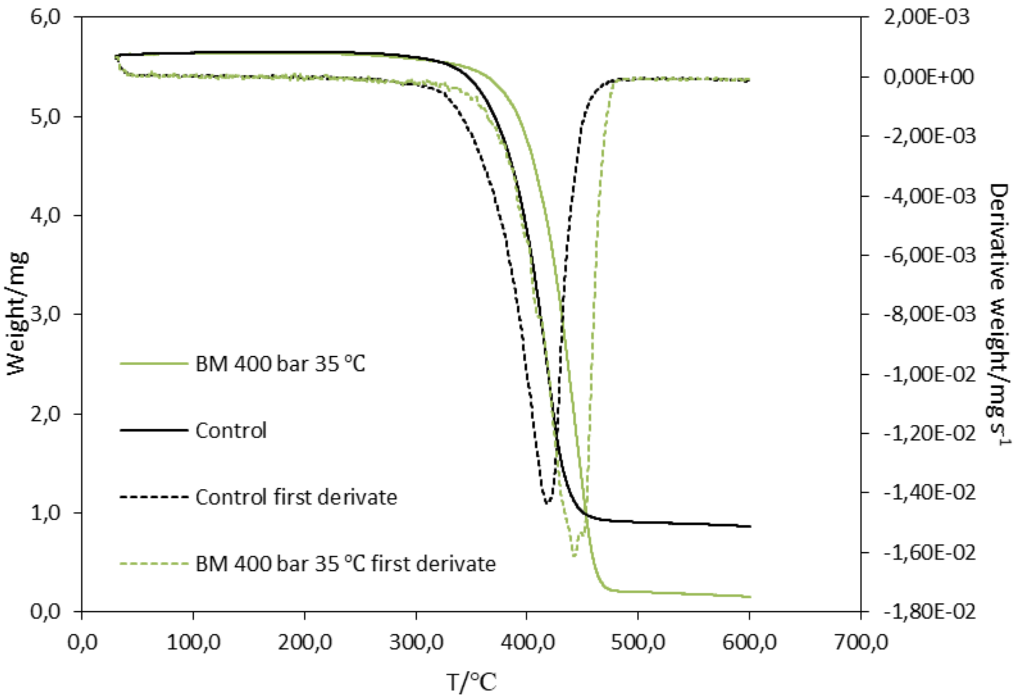

Figure 4. TGA thermograms and first derivative plots of control sample (non-treated PET/PP multilayer film) and PET/PP laminate film impregnated with OLE by the BM process at 400 bar and 35°C.

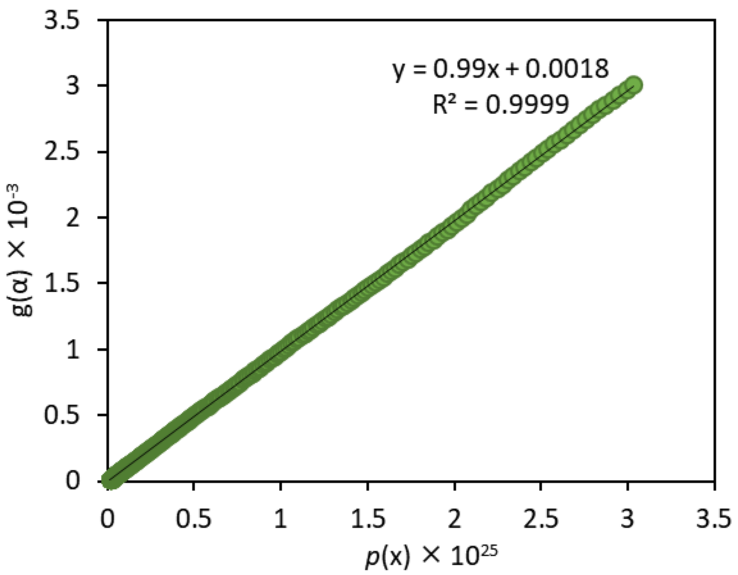

Figure 5. Plots of $g(\alpha)$ versus $p(x)$ for the three-dimensional diffusion (D3) fitting of PET/PP laminate film sample impregnated with OLE by the BM process at 400 bar and 35°C.